Industrial Crops and Products xxx (2015) xxx–xxx

Contents lists available at ScienceDirect

Industrial Crops and Products

journal homepage: www.elsevier.com/locate/indcrop

Nanofibrillar cellulose from *Posidonia oceanica*: Properties and morphological features

F. Bettaieb[a,b,c], R. Khiari[a,b,c,**], A. Dufresne[b,c], M.F. Mhenni[a], J.L. Putaux[d], S. Boufi[e,*]

[a] *Research Unity of Applied Chemistry & Environment, Department of Chemistry, Faculty of Sciences, University of Monastir, 5019 Tunisia*
[b] *University Grenoble Alpes, LGP2, F-38000 Grenoble, France*
[c] *CNRS, LGP2, F-38000 Grenoble, France*
[d] *CERMAV, UPR CNRS 5301, ICMG FR 2607, BP 53, Grenoble Cedex 9, France*
[e] *University of Sfax-Faculty of Science – LMSE, Tunisia*

ARTICLE INFO

Article history:
Received 31 October 2014
Received in revised form 1 December 2014
Accepted 27 December 2014
Available online xxx

Keywords:
Posidonia oceanica balls and leaves
Polymer matrix composite
Mechanical properties

ABSTRACT

Posidonia oceanica a dominant Mediterranean Sea grass was used as a starting material to produce nanofibrillar cellulose. Thus, NFC gel was produced by the disintegration in a high pressure homogenizer of cellulose pulp extracted from *P. oceanica*. The ensuing NFC suspension was characterized in terms of fibrillation yield, transparency, rheological behavior and morphological features. The reinforcing potential of the ensuing NFC was also investigated using dynamic mechanical analysis (DMA) from measurements carried out on nanocomposites films prepared by casting a mixture of NFC suspension and commercial acrylic latex. The prepared materials have showed promising mechanical properties.

1. Introduction

Over the last decades, cellulosic fibers were widely used for several fields from different sectors such as the building products, furniture industries, pulp and paper industry, as well as for the preparation of innovative materials such as 'green' composites. As a consequence, the utilization of cellulosic fibers is intensifying, and it is becoming more and more difficult to satisfy the large demand and makes it challenging to supply all users with the needs and at reasonable cost. This is the reason why, non-wood species and the annual plants can be considered as alternative sources of cellulosic fibers, especially in forest-poor regions. Moreover, non-wood fibers and/or annual plants are often obtained from agricultural wastes and can therefore be valorized providing them an added-value. There are many reports examining the use of annual plants or/and non-wood wastes as a new raw material to produce fibers (Aguir and Mhenni, 2006, 2007; Belgacem et al., 1986; Douissa et al., 2013; Ncibi et al., 2008; Khiari et al., 2010). These strategies were already applied in various countries such as: Portugal (Antunes et al., 2000; Abrantes et al., 2007; Cordeiro et al., 2004), India (Dutt et al., 2005, 2008), Malaysia (Chia et al., 2008; Rosli et al., 2003), Iran (Hedjazi et al., 2008) or Tunisia (Belgacem et al., 1986; Khiari et al., 2010, 2011a,b) and so on.

Nanofibrillar cellulose which is also called cellulose microfibril and/or microfibrillar cellulose and/or more currently, nanofibrillated cellulose (NFC), has been the subject of intense research activities, mainly in areas of nanocomposite applications (Kalia et al., 2014; Klemm et al., 2005; Siqueira et al., 2010a; Siró and Plackett, 2008). The nanofibrillar cellulose (NFC) was originally developed by Turbak et al. in the 1980s by using high pressure homogenization of wood fibers in water suspension. The NFC has been isolated from different lignocellulosic materials using different mechanical technologies such as high-pressure homogenizers (Alila et al., 2013; Andresen et al., 2006; Andresen and Stenius, 2007; Djafari Petroudy et al., 2014; Erkisen et al., 2008; Herrick et al., 1983; Nakagaito and Yano, 2004; Rezayati Charani et al., 2013; Stenstad et al., 2008; Syverud and Stenius, 2009; Turbak et al., 1983; Winuprasith and Suphantharika, 2013; Zhang et al., 2012), micro-fluidizers (Bendahou et al., 2010), ultrafine grinders (Abe et al., 2007; Abe and Yano, 2009; Hassan et al., 2012; Iwamoto et al., 2005, 2008; Jang et al., 2013; Subramanian et al., 2008), cryo-crushing (Chakraborty et al., 2005; Janardhnan and Sain, 2006), and ultrasonic method (Zhao et al., 2007). In all case, the isolation of nanofibrillar cellulose from the fibers was implemented using high shear force that makes easy the separation of the fibrils. In fact,

* Corresponding author.
** Corresponding author at: Research Unity of Applied Chemistry & Environment, Department of Chemistry, Faculty of Sciences, University of Monastir, 5019 Tunisia. Tel.: +216 20060004; fax: +216 73500278.
E-mail addresses: khiari_ramzi2000@yahoo.fr (R. Khiari), Sami.boufi@fss.rnu.tn (S. Boufi).

http://dx.doi.org/10.1016/j.indcrop.2014.12.060
0926-6690/

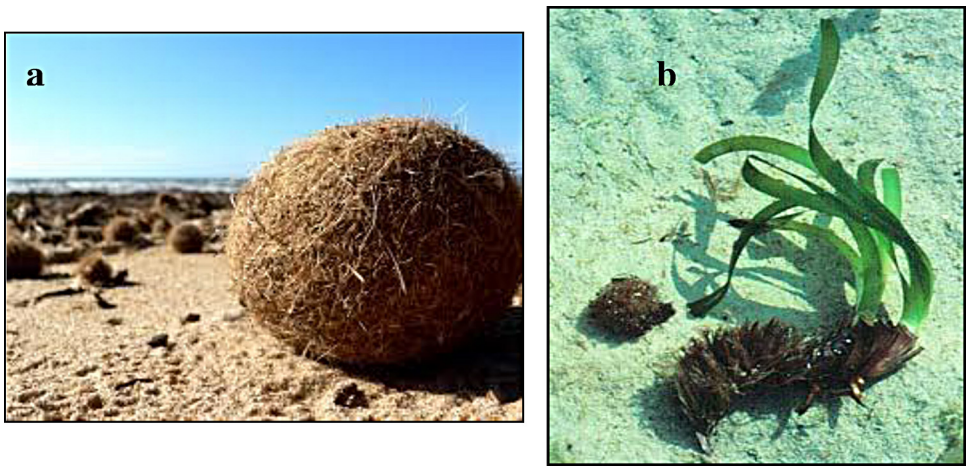

Fig. 1. *P. oceanica* balls (a) and leaves (b).

the isolation of the nanofibers is energy intensive and therefore pre-treatments of the fibers prior to the isolation of the nanofibers have been studied. In this context, it has been shown that chemical pre-treatment such as swelling in alkali solutions facilitates the isolation of nanofibrillar cellulose (Hassan et al., 2010). TEMPO (2,2,6,6-tetramethylpiperidine-1-oxyl) oxidation was also used as a pre-treatment before mechanical treatment for nanofibers isolation (Saito et al., 2006). In the literature, there are reports of cellulose microfibril extraction from diverse non-wood sources including wheat straw and soy hulls (Alemdar and Sain, 2008), sugar beet pulp (Dufresne et al., 1997; Dinand et al., 1996, 1999; Gousse et al., 2004; Habibi and Vignon 2008), potato pulp (Dufresne et al., 2000), swede root (Bruce et al., 2005), bagasse (Bhattacharya et al., 2008), sisal (Moran et al., 2008), algae (Imai et al., 2003), stems of cacti (Habibi et al., 2009; Malainine et al., 2005), rice straw and rapeseed (Chaker et al., 2014a), Triticale crops (Boufi and Gandini, 2015) and banana rachis (Zuluaga et al., 2009). These reports were focused on the preparation of NFC and its applications. The same strategy could be applied for many Tunisian cellulosic residues such as the *Posidonia oceanica* balls and leaves (Fig. 1). This plant is the dominant Mediterranean Sea grass. Important quantities of *P. oceanica* fragments accumulate on Tunisian coasts, imposing the necessity of cleaning the beaches. The investigation of this available and renewable lignocellulosic biomass can be considered as a suitable solution for this problem. Nowadays, *P. oceanica* is studied as a low cost and renewable adsorbent for removing dyes or phenol (Ncibi et al., 2006a,b, 2008; Gezguez et al., 2009) or as a source of cellulose (Aguir and Mhenni, 2006; Khiari et al., 2010, 2011a,b). To the best of our knowledge, no data about the preparation of NFC from *P. oceanica* are available in the literature. Consequently, this work is devoted to the isolation and characterizing the NFC from *P. oceanica*. Fist, cellulose is isolated and then chemically pre-treated using TEMPO oxidation prior to the mechanical treatment in order to facilitate the preparation of the NFC. The isolated NFC was used to prepare NFC-reinforced nanocomposites based on rubber matrix.

2. Materials and methods

2.1. Raw materials

The *P. oceanica* (as raw material) balls and leaves (R-POB and R-POL) were obtained from Skanes-Monastir (Tunisia) in April 2013 and were dried under natural conditions (average relative humidity: 65%; average temperature: around 25 °C). Then, they were washed several times in order to eliminate sand and contaminations before being used. All chemicals and reagents utilized in this work were purchased from Sigma–Aldrich and were used without further purification. The polymer acrylic latex dispersion was a commercial product from MPC-PROKIM (Tunisia). It consists of styrene (S – 35 wt%) and butyl acrylate (BA – 5 wt%). The size of the polymer particles was around 140 nm, the glass transition around 30 °C and the solid content 50 wt%.

2.2. Preparation of cellulose and cellulose microfibrils and nanocomposites

Fig. 2 illustrates the isolation pathways leading to the preparation of different nanofibrillar cellulose from the two studied raw materials.

2.2.1. Delignification and bleaching of pulp

The delignification and the bleaching procedures of cellulose from *P. oceanica* can be briefly described, as follows: the preparation of extracted-bleached cellulose is conducted in two steps. The R-POL or R-POB is dispersed in a 2% aqueous soda solution (2 wt%). This delignification is performed at 80 °C and followed by filtration and washing with distilled water until neutral pH. The obtained residues were then bleached using a sodium chlorite

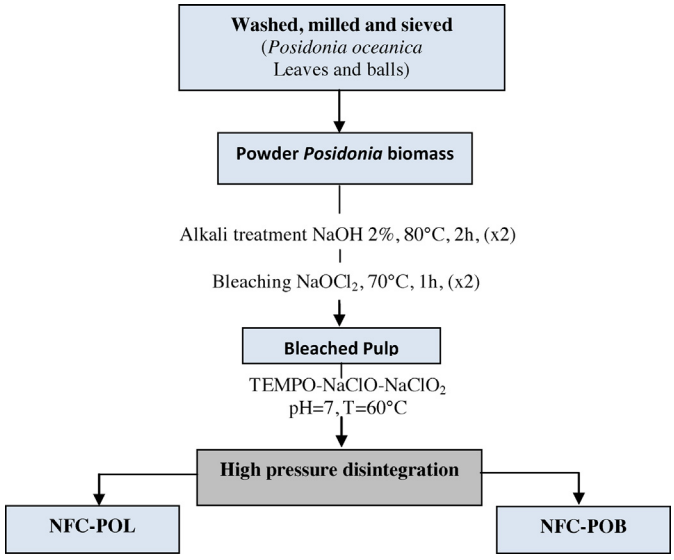

Fig. 2. Schematic representation of the different steps used to produce different NFC.

Please cite this article in press as: Bettaieb, F., et al., Nanofibrillar cellulose from *Posidonia oceanica*: Properties and morphological features. Ind. Crops Prod. (2015), http://dx.doi.org/10.1016/j.indcrop.2014.12.060

($NaClO_2$) solution in a buffer medium under mechanical stirring following a well-established method (Wise et al., 1946). The obtained fibers from *P. oceanica* balls and leaves are called, F-POB and F-POL, respectively. Each delignification- bleaching condition was carried out, at least in duplicate and the difference between the obtained yields was within an experimental error of 5%.

2.2.2. TEMPO-mediated oxidation of pulp

The procedure and reagent ratios used by Besbes et al. (2011a,b) were applied for TEMPO-mediated oxidation of cellulose fibers. About 5 g of pulp from *P. oceanica* leaves or balls were dispersed in 500 mL sodium phosphate buffer (0.05 mol L^{-1}, pH 7) containing 100 mg of TEMPO. Then, 3 g of sodium chlorite (80%) and 3 ml of sodium hypochlorite solution (2 mol L^{-1}) were added and the suspension was left under magnetic stirring at 60 °C during 6 h. During the oxidation process, the color of the modified pulps turned into yellow as a result of the generation of free chlorine. At the end of the oxidation reaction, 100 mL of ethanol was added and the obtained modified fibers were filtered and washed several time with deionized water.

2.2.3. Homogenization of pulp

After oxidation pre-treatment of prepared fibers from *P. oceanica* balls and leaves (F-POB and F-POL), a 1–2% fiber suspension in water was homogenized with high pressure homogenizer (NS1001L PANDA 2K-GEA). The disintegration process was first carried out by passing the fiber suspension at a pressure of 300 bar for about 5 passes until the suspension turned to a gel. Then, the gel was further homogenized with about five additional passes at 600 bar, to ensure high level of disintegration.

Due to the excessive shearing action during the homogenization process, the temperature of the suspension increased up to 60–70 °C.

2.3. Preparation of nanocomposites

Cellulose microfibril suspensions were mixed with latex matrix (commercial latex of poly(styrene-co-butyl acrylate) in various amounts in order to prepare composite films containing different loadings, namely 0, 1, 2, 5, 7, 10 and 15% (w/w with respect to the matrix). After stirring, the ensuing materials were prepared by casting the mixture in a Teflon mould and stored at 35 °C. The samples were conditioned for 24 h in conditioned room, under controlled temperature (23 °C) and relative humidity (50%).

2.4. Characterization

Several methods were used to characterize the raw materials or the prepared NFC suspensions.

2.4.1. Carboxyl content on oxidizied NFC-conductimetric titration

The conductimetric titration was performed to determine the carboxyl content of oxidized cellulose samples. The oxidized cellulose was suspended into 15 mL of hydrochloric acid (0.01 mol L^{-1}) solutions. After 30 min of stirring, the suspension was titrated with a solution of sodium hydroxide solution (0.01 mol L^{-1}). The titration curves showed the presence of a strong acid (V_a corresponding to the excess of HCl and a weak one (V_b) associated with the carboxyl content). This parameter was determined from the following Eq. (1):

$$n(\mathrm{COOH}) = 0.01 \times (V_2 - V_1) \times 0.0 \quad (1)$$

The measurements were repeated at least in duplicate and the difference between the various values obtained was within an experimental error of 5%.

2.4.2. Yield of fibrillation

As described by Alila et al. (2013) and Benhamou et al. (2014), a dilute suspension having about 0.2% of solid content (Sc) was centrifuged at 4000 rpm during 30 min to separate the fibrillation material (in supernatant fraction) from the non-fibrillated and/or partially fibrillated ones (the sediment). This fraction was dried at 90 °C in a halogen desiccator until a constant weight. The yield of the nanofibrillated was determined as follow from Eq. (2):

$$\text{Yield of fibralltion}(\%) = 100 \times \left(1 - \frac{\text{weight of dried sediment}}{\text{weight of diluted sample} \times \%\mathrm{Sc}}\right) \quad (2)$$

where, Sc%, solid content of the diluted dispersion sample. The measurement was repeated at least in duplicate and the difference between the various values obtained was within an experimental error of 5%.

2.4.3. X-ray diffraction analysis

The crystallinity of the cellulosic materials was studied by X-ray diffraction (XRD). The following materials were investigated: R-POL, R-POB, F-POL, F-POB, NFC–POL and NFC–POB. Each material in the form of milled powder was placed on the sample holder and leveled off to obtain total and uniform X-ray exposure. The obtained samples were examined using an X-ray diffractometer (D8-Advance Bruker AXS GmbH) at room temperature with a monochromatic CuKα radiation source (λ = 0.154 nm) in step-scan mode with a 2θ angle ranging from 5° to 60° with a step of 0.04 and a scanning time of 5.0 min. The method of Segal et al. (1959) was considered to evaluate the crystallinity of the different prepared samples. The crystallinity index C_I was determined based on the reflected intensity data following (Eq. (3)):

$$C_I(\%) = 100 \times \left(\frac{I_{002} - I_{\mathrm{am}}}{I_{002}}\right) \quad \text{Eq.3}$$

where: I_{002} is the maximum intensity of the (0 0 2) lattice diffraction peak and I_{am} is the intensity scattered by the amorphous part of the sample. The diffraction peak for plane (0 0 2) is located at a diffraction angle around 2θ = 22° and the intensity scattered by the amorphous part is measured as the lowest intensity at a diffraction angle around 2θ = 18°.

2.4.4. Transmission electron microscopy (TEM)

About 0.5 μL of each suspension of NFC was loaded onto a 300 mesh carbon coated formvar copper grids using a labnet micropipette. Water in the suspensions on the carbon coated grids was allowed to evaporate. Additional drop of each cellulose NFC suspension was added onto their respective grids to increase the amount of cellulose particles and the process was repeated several times. NFC coated grids were examined using JEOL 200CX transmission electron microscope at 80 kV.

2.4.5. Optical transmittance

The optical properties of the prepared NFC were studied by a Cecil, CE1010UV via spectrometer. NFC water suspension was introduced in a quartz cuvette and the transmittance was measured from 400 to 800 nm. A cuvette filled with distilled water was used as reference. The measurement was repeated at least in duplicate and the difference between the various values obtained was within an experimental error of 5%.

2.4.6. Rheological measurement

The rheological behavior of NFC–POL and NFC–POB suspensions was studied using a controlled speed rotating rheometer (Anton Paar MCR301). The tests were carried out at 20 °C. Shearing tests were performed with cone-plate geometries.

Please cite this article in press as: Bettaieb, F., et al., Nanofibrillar cellulose from *Posidonia oceanica*: Properties and morphological features. Ind. Crops Prod. (2015), http://dx.doi.org/10.1016/j.indcrop.2014.12.060

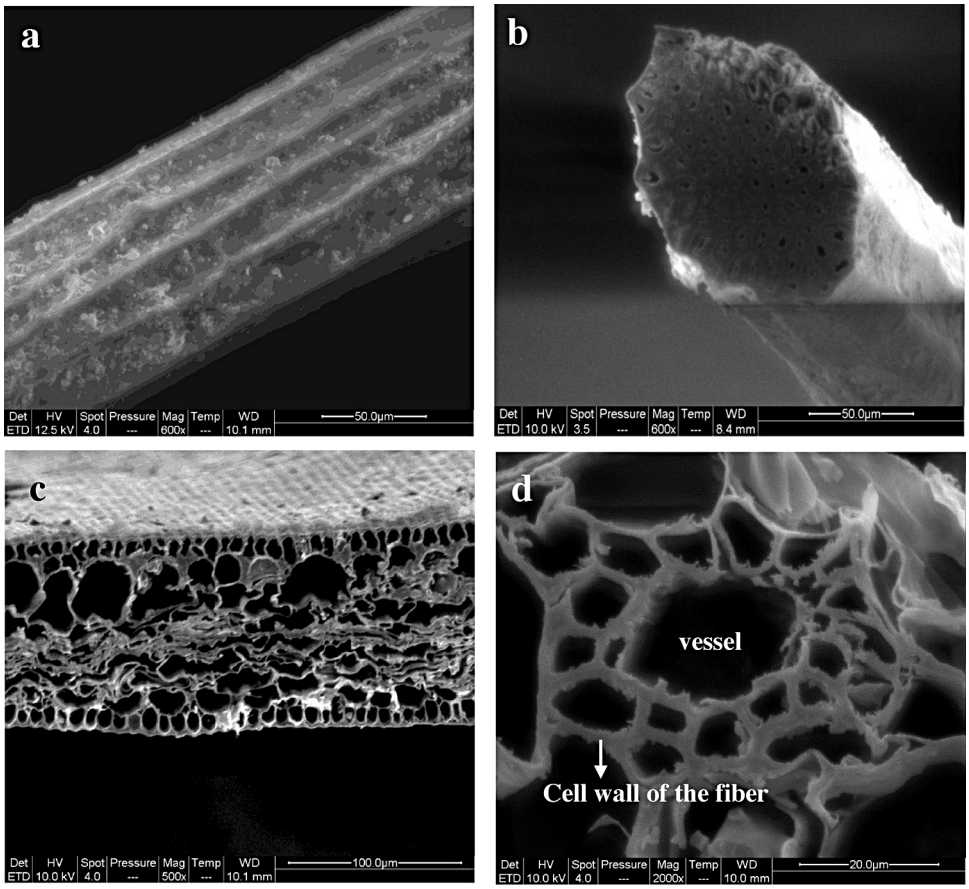

Fig. 3. Macroscopic observation of the *P. oceanica* balls (a–b) leaves (c–d).

2.4.7. Dynamic mechanical analysis

Dynamic mechanical analysis (DMA) experiments were conducted in tension mode using a PYRIS Diamond DMA (Perkin–Elmer, Waltham, MA, USA). Temperature scans were run from −50 °C to 100 °C at a heating rate of 2 °C min^{-1}, a frequency of 1 Hz and an amplitude of 10 μm. The storage modulus(E') as well as the loss factor tan δ were measured as a function of temperature. Sample dimensions were about 20 mm (length), 5 mm (width) and 0.1–0.3 mm (thickness).

3. Results and discussions

3.1. Fibers characterization

The general aspect of R-POL and R-POB was examined with a scanning electron microscope at different magnifications. Surface, longitudinal views as well as cross sections of the investigated raw materials are given in Fig. 3. It is obvious to conclude that *P. oceanica* leaves (Fig. 3c and d) present very porous structure compared with that of *P. oceanica* balls (Fig. 3a and b).

The *P. oceanica* balls were composed mainly of sclereid cell (or fibers) with about 20 μm in diameter and a wall having about 10 μm of thickness. On the other hand, several different cell elements, namely parenchyma, vascular tissue, epidermis, and the fiber cells can be seen in case of *P. oceanica* leaves. The fibers displayed a large lumen width (in the range of 10–20 μm) and cell walls thickness between 2 and 5 μm, depending on their position in the leaf, the outer cells being thicker than the inner ones.

The chemical compositions of POB and POL prior and after chemical pulping are given in Table 1. Native R-POB and R-POL were composed of cellulose, hemicelluloses, lignin and ash. After $NaClO_2$ pulping process, lignin was completely removed and a high fraction of hemicelluloses was left in the fibers, which is in agreement with the specificity of $NaClO_2$ action. Thus, this reagent is capable to remove selectively lignin, with low incidence on hemicelluloses. $NaClO_2$ delignification led to the effective removal of lignin, with the highest yield around 65%. The ensuing pulp was white, without any necessity to implement a bleaching treatment. However, a fraction of mineral compounds remained in the fibers after the pulping process.

The XRD diffraction patterns of R-POB and R-POL are given in Fig. 4.

The typical cellulose I structure was observed in the diffraction pattern for each starting materials. It has strong crystalline peaks at 16° and 22° corresponding to the (1 1 0) and (0 0 2) planes of crystals, and weak crystalline peaks at 34.8° to the (0 0 4) plane (Isogai et al., 1989; Liu et al., 2005; Oh et al., 2005). However, two other mineral compounds were also present, namely silica (SiO_2) and weddellite (CaC_2O_4–$2H_2O$) which is a form of calcium oxalate. It can be noticed also from the Fig. 4 that the intensity of weddelite was more important in the case R-POB than R-POL. The presence of these mineral salts is typical in sea biomass and accounts for the high ash content, more specifically for POB. The C_I for R-POB and R-POL was about 52% and 41%, respectively.

After the pulping process, the cellulose I form was preserved. The XRD characterization revealed the presence of the main characteristic peaks of cellulose I at 2θ values of 15.5° and 22.2°, for all studied samples, before and after the extraction procedure, indicating the preservation of the native crystalline structure even in the presence of the NaOH treatment. After lignin extraction, the crystallinity index increased due to the partial removal of the amorphous hemicelluloses and lignin. In addition, lower C_I was found for

Please cite this article in press as: Bettaieb, F., et al., Nanofibrillar cellulose from *Posidonia oceanica*: Properties and morphological features. Ind. Crops Prod. (2015), http://dx.doi.org/10.1016/j.indcrop.2014.12.060

Table 1
Chemical analysis of POL and POB.

	Ash, %	Klason lignin,%	Hollocellulose, %	α-cellulose, %	Morphology		C_I, %
					Width (μm)	Length (mm)	
R-POB	12	29.8	61.8	40	–	–	52
R-POL	5	24.7	57.1	31.4	–	–	41
F-POB	7.4	0.3	92.3	72	21.3	0.55	58.4
F-POL	3.5	1.4	95.1	79	27	0.69	52.6
NFC–POB	–	–	–	–	5*–21*	752*	63.5
NFC–POL	–	–	–	–	2*–15*	1043*	52.9

R-POB: Raw *P. oceanica* balls, F-POB: *P. oceanica* fibers from balls.
R-POL: Raw *P. oceanica* leaves, F-POL: *P. oceanica* fibers from leaves.
* nm as unity for the width of NFC from POB and POL.

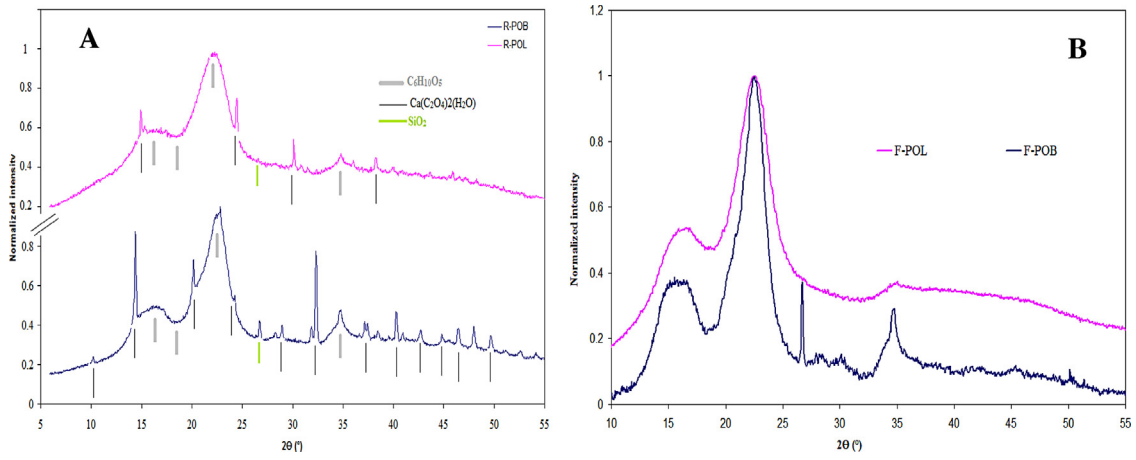

Fig. 4. XRD spectra of (A): raw *P. oceanica* balls (R-POB) and raw *P. oceanica* leaves (R-POL) and (B): fiber *P. oceanica* balls (F-POB) and fiber *P. oceanica* leaves (F-POL).

F-POL, presumably due to the lower cellulose content in POL and higher hemicellulose content.

After the pulping process, individualized fibers having a width in the range of 20–25 μm were obtained (Fig. 5). The mean length and width of the delignified fibers, determined from MORFI analysis, were around 500–600 μm and 20 μm, respectively.

3.2. NFC preparation and characterization from P. oceanica leaves and balls

TEMPO-mediated oxidation of F-POB and F-POL fibers was adopted in order to facilitate the defibrillation process and reduces the energy demand during the homogenization process. Referring to literature data, 300 μmol g^{-1} of ionic groups is a minimal level in order to perceive an effect on the fibrillation behavior (Besbes et al., 2011). In our case, the oxidation of the fibers was implemented to enhance the carboxyl content up to about 500 μmol g^{-1}, and the fibers were disintegrated in a high pressure homogenizer for 10 passes (5 passes at 30 MPa Bar followed by 5 additional passes at 60 MPa). The fibrillation yield for NFC–POB and NFC–POL was about 73% and 58%, respectively.

One important result to highlight is the meaningful difference in the fibrillation yield between POB and POL (73% for POB against 58% for POL), albeit the similar approach adopted for the production of NFC, both in terms of the pre-treatment as well as concerning the number of passes and the pressure of disintegration. This result points out that fibers from POL were harder to be broken down into nanosized fibrils than those from POB. Further evidence of the difference in the fibrillation behavior is provided from the higher transparency of the NFC gel from POB compared to that from POL (Fig. 6). The transmittance of the NFC gel from POB ranged from 30 to 50% while that from NFC–POL is around 20%. The decrease in the optical transparency of the NFC gel is brought by light scattering against microsized fibrils. Accordingly, the higher the content of partially or non-fibrillated material the more intense is the light scattering and the lower is the transparency of the NFC-gel. Moreover, NFC gel from POB showed stronger dependence of transmittance with wavelength (lower transmittance at shorter wave lengths) than gel from POL which is a further indication of the higher fraction in nanosized fibrils. Indeed, for nanoparticles with square section lower than 50 nm, the light scattering is inversely proportional to the fourth power of wavelength. $I \propto 1/\lambda^4$ (Ganikhanov et al., 2006).

The difference in the fibrillation properties of NFC–POB and NFC–POL is assigned to the difference in their chemical composition and more specifically to the higher hemicelluloses content in fibers from POB (about 22% for POB against 16% for POL). This factor was recently reported to exert a key role in the fibrillation efficiency of the cellulose fibers. The higher the hemicelluloses content, the easier is the breakdown of the cell wall to release cellulose microfibrils. It was assumed that hemicelluloses spanning the gap between the microfibrils, behave as a physical barrier preventing the microfibrils from coming into close contact thus reducing their mutual interaction through hydrogen bonding (Chaker et al., 2014a,b).

NFC suspension is known to exhibit gel-like aspect as the solid content exceeds a critical threshold in the range of 0.5–1%, depending on the origin and the morphological features of the cellulose nanofibrils. The evolution of the viscosity versus shear rate of NFC from POB and POF is shown in Fig. 7. Both the NFC suspension showed strong shear thinning behavior as attested by the intense decrease in the viscosity as the shear rate is increasing. For instance, the viscosity of the NFC gel from POB falls down from 225 to about 15 Pa s, as the shear rate goes from 0.1 to 2 s^{-1}. This behavior, typical of NFC dispersion, is explained by the hydrodynamic properties of charged cellulose nanofibrils with high aspect ratio. The presence of

Please cite this article in press as: Bettaieb, F., et al., Nanofibrillar cellulose from *Posidonia oceanica*: Properties and morphological features. Ind. Crops Prod. (2015), http://dx.doi.org/10.1016/j.indcrop.2014.12.060

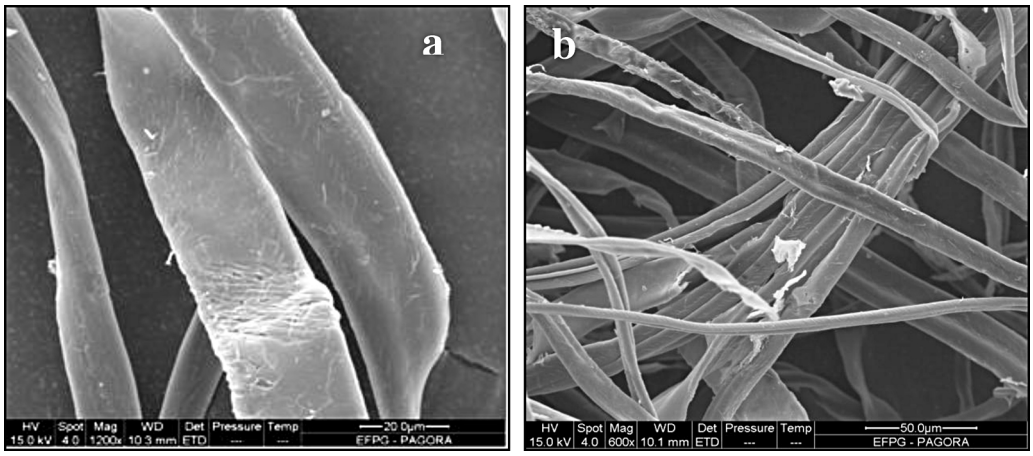

Fig. 5. SEM observation of bleached fibres obtained from F-POL (a) and F-POB (b).

ionized carboxyl groups on the surface of the nanofibrils generated an electric double layer surrounding the nanofibrils that prevented the nanofibrils from aggregation induced by hydrogen bonding and van der Waals interaction. Upon the application of a shear rate the network is progressively broken down, the elementary nanofibrils start to be oriented in the shear direction leading to their disentanglement. As a consequence, the flow resistance is lowered and the viscosity is decreased. This explains the strong fall in the viscosity values as the NFC gel is sheared. Once in rest, the nanofibrils network is reformed and the viscosity regained its original value. However, as seen in Fig. 7, NFC–POB gel looks more viscous than NFC–POL. At a given shear strain, the viscosity of NFC–POB gel is about two times higher than that of NFC–POL. The difference in the consistency of the NFC gel is likely to the difference in the fibrillation yield between the NFC from POB and POL (73% for POB against 58% for POL). The higher the content in nanofibrillated material, the more viscous is the ensuing gel. Though, other parameters, such as the morphological features of the NFC (in terms of length and width), surface charge groups and pH affected also the rheological properties of NFC gel.

3.2.1. Morphology of NFC

The morphological features of NFC produced from *P. oceanica* leaves and balls were assessed by TEM observations (Fig. 8). The observation revealed nanosized fibrils with wide heterogeneous distribution both in width and in length. The dimensions of the corresponding nanofibrils were evaluated by digital image analysis (Image J) of TEM micrographs using a minimum of 90 nanofibrils. Data indicated broad width distribution of the nanofibrils ranging from 5 up to 21 nm for NFC from POB and from 2 to 15 nm for NFC from POL. The individual fibrils with width lower than 5 nm corresponded presumably to elementary cellulose fibrils composed of altering crystalline and amorphous domains. On the other hand, the larger fibrils are likely composed of bundles of elementary fibrils blinded together through hydrogen bonding.

Table 2 summarizes the morphological features of NFC from different species. The value of NFC–POB is typically in the aspect ratio range of NFC regardless the cellulose source and the growth conditions (Dufresne, 2012). These observations are similar to those reported for sugar beet (Dinand et al., 1996, 1999; Dufresne et al., 1997), potato pulp (Dufresne et al., 2000), algae (Imai et al., 2003), cladodes (Malainine et al., 2005) and peel of prickly pear fruit

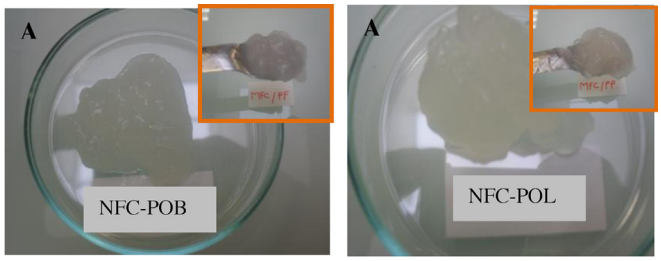

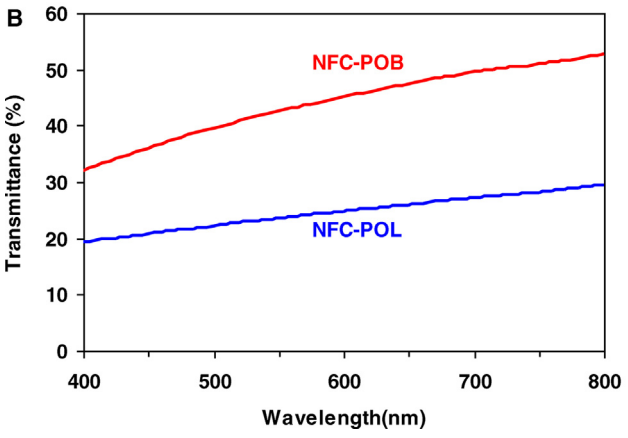

Fig. 6. (A) Digital photos of NFC gel at 1 wt% and (B) UV–vis transimittance spectra of the NFC–POL and NFC–POB suspension'.

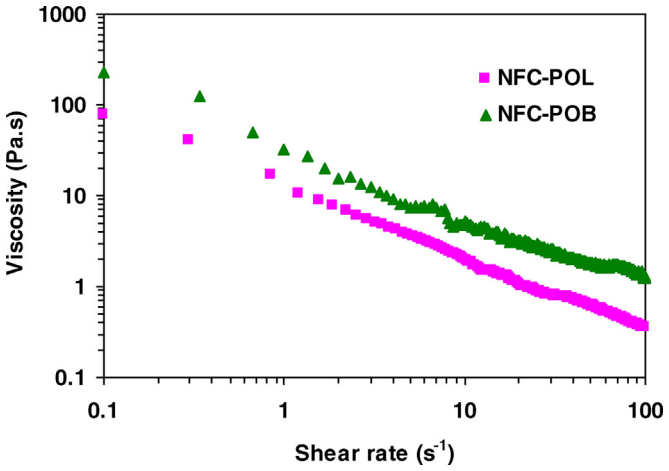

Fig. 7. Viscosity as a function of shear rate of the NFC gel at 1.5 wt.% solid content.

Please cite this article in press as: Bettaieb, F., et al., Nanofibrillar cellulose from *Posidonia oceanica*: Properties and morphological features. Ind. Crops Prod. (2015), http://dx.doi.org/10.1016/j.indcrop.2014.12.060

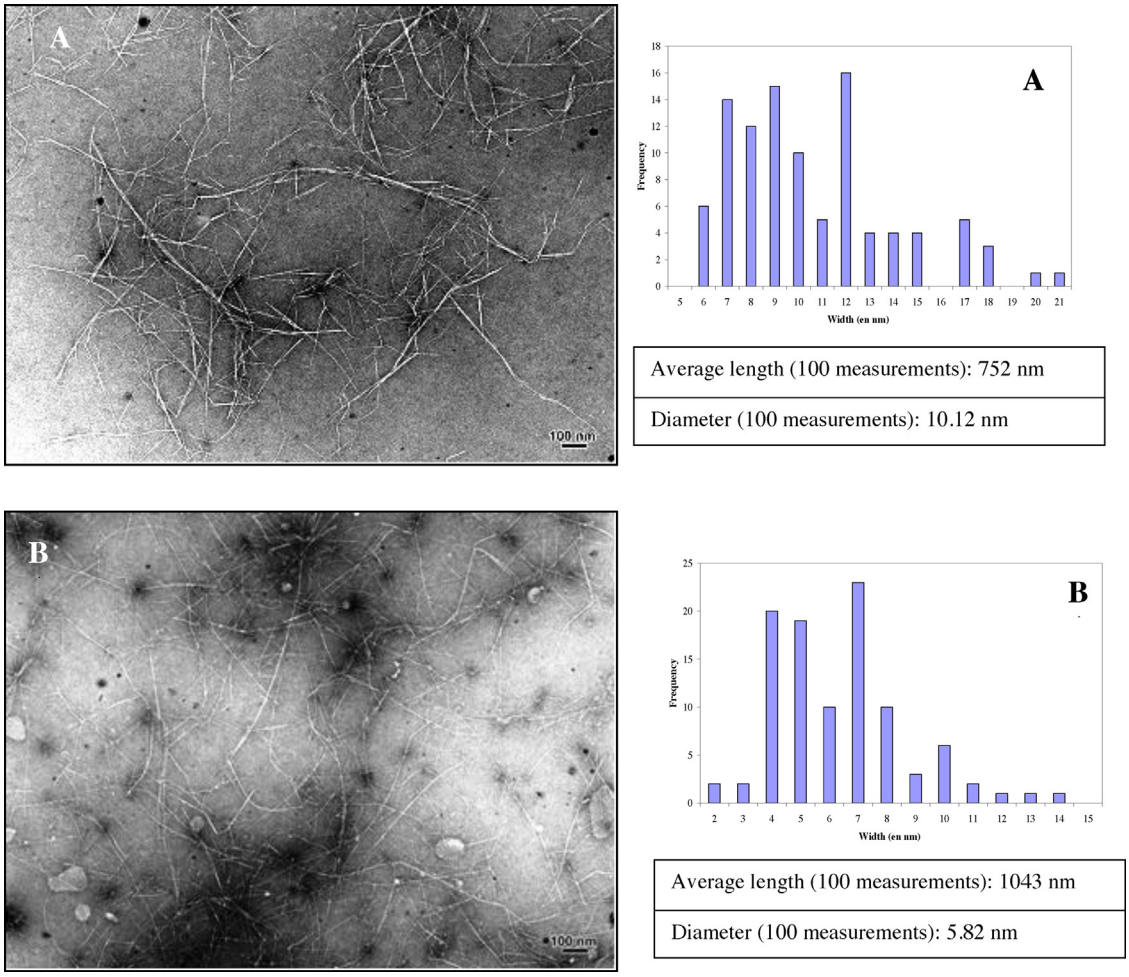

Fig. 8. TEM observations and diameter distribution of the NFC–POB (A) and NFC–POL (B).

(Habibi et al., 2009) of *Opuntia ficus-indica*, a cactus, swede root (Bruce et al., 2005), hemp (Wang and Mohini, 2007), rachis date palm (Bendahou et al., 2009), and many others. However in the case of NFC–POL, the morphology is similar to Tunicin (Dufresne, 2012) which presents a low diameter and very large length. In all case the high aspect ratio of the NFC obtained from *P. oceanica* indicates that these structures exhibit promising behavior as cellulose microfibrils for polymer matrices, providing valorization of this worldwide produced agricultural waste.

3.3. Dynamic mechanical analysis (DMA) of the nanocomposites film

The reinforcing potential of NFC from *P. oceanica* was investigated by DMA. An example of the evolution of the storage modulus E' as a function of temperature for different nanofiller contents is shown in Fig. 9 for NFC prepared from POB. As expected, the effect of the inclusion of NFC into the polymer matrix differs depending on the temperature range. Below the glass transition temperature,

Table 2
Width values of NFC produced via high-pressure homogenization and TEMPO-mediated oxidation.

Starting materials	Width (nm)	Reference
Banana Rachis	5–60	Zuluaga et al. 2009
Corn cobs	5–60	Dufresne, 2012
Date palm rachis	5–10	Bendahou et al. 2009, 2010
Opuntia ficus indica	5	Malainine et al. 2005
Rubberwood	10–90	Jonoobi et al., 2011
Sisal	52 ± 15	Siqueira et al. 2010b
Kenaf	10–90	Jonoobi et al. 2009
Tunicin	5–20	Saito et al. 2006
Cotton	5–20	Saito et al. 2006
Empty fruit bunches of oil palm	5–40	Jonoobi et al. 2011
Potato Pulp	5	Dufresne et al. 2000
Maize Bran	5–20	Rondeau-Mouro et al. 2003
Bacterial cellulose	3–100	Saito et al. 2006
Kraft pulp	5–20	Fukuzumi et al. 2009; Besbes et al., 2011b
Sugaracane Bagasse	30	Bhattacharya et al. 2008
Corn stalk	5–10	Chaker et al. 2014a
Rapeseed straw	5–10	Chaker et al. 2014a

Please cite this article in press as: Bettaieb, F., et al., Nanofibrillar cellulose from *Posidonia oceanica*: Properties and morphological features. Ind. Crops Prod. (2015), http://dx.doi.org/10.1016/j.indcrop.2014.12.060

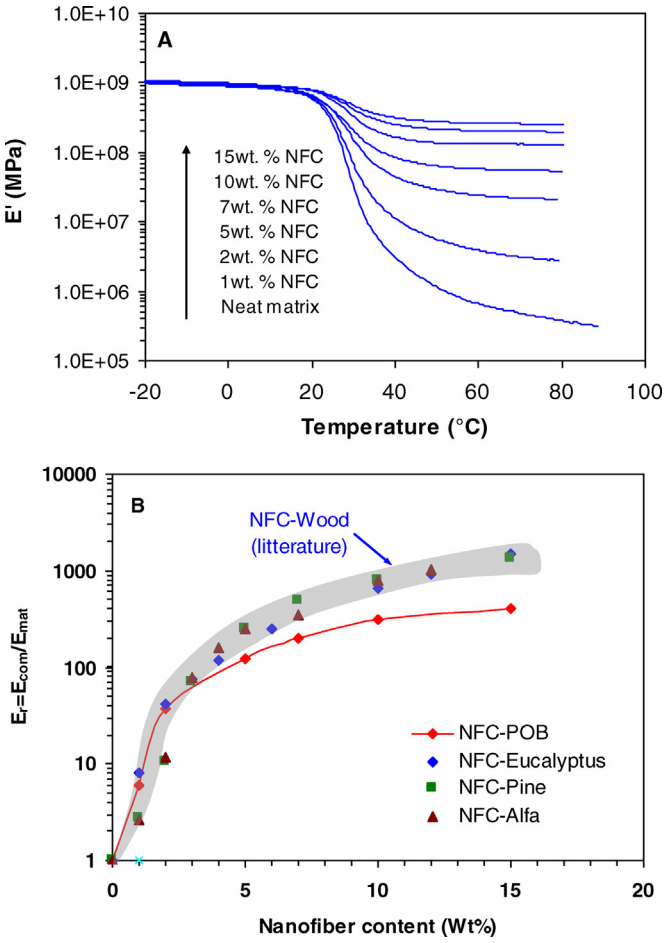

Fig. 9. Evolution of (A) the storage tensile modulus, E, versus temperature at 1 Hz for nanocomposites based on NFC from POB, and (B) the relative storage modulus $E_r = E_c/E_{mat}$ versus NFC content at 70 °C.

no significant evolution in the storage modulus is detected upon the addition of NFC. On the other hand, above the glass transition the storage modulus is more sensitive to the presence of the nanofiller and increased significantly with NFC addition, in line with the well-known reinforcing effect of cellulose based nanofibrils (Dufresne, 2010). This means that the cellulose nanofibrils are most effective in restricting the mobility of the polymers chains above *Tg*. The strong reinforcing potential above the glass transition is ascribed to the set-up of a rigid entangled held through hydrogen interaction in the bonded area.

To better highlight the reinforcing effect of the different cellulosic nanofillers, the evolution of the storage modulus E' of the nanocomposites in the rubbery state (estimated at 70 °C) versus nanofiller content was plotted in Fig. 9b. The results show a significant rise in the storage modulus with nanofiller addition, in agreement with the strong reinforcing potential of NFC. For instance, at 70 °C the nanocomposite containing 5 and 10 wt% NFC exhibits a storage modulus around 25 MPa and 60 MPa, respectively, which represents 450 and 195-folds enhancement, respectively, with respect to that of the neat matrix (0.133 MPa).

For sake of comparison, data collected from literature for nanocomposite prepared from acrylic and NFC from wood and annual plant, and adopting the same mixing route were included in the graph. The relative modulus extracted from the literature data was determined at the same temperature of 70 °C. It is interesting to note that below 5% NFC, the increment in the modulus was nearly similar to the nanocomposite films prepared from wood based NFC. On the other hand, over this content, the trend is inversed and the stiffening effect brought by the NFC from POB was lower than that wood fibers. We rationalize this divergence to the difference in the nanofibrils morphology, more specifically to the lower length of the cellulose nanofibrils from POB compared to that from wood.

4. Conclusion

During this work, cellulose nanofibers were successfully isolated from *P. oceanica* balls and leaves (POB and POL) by chemical treatments followed by homogenization process. The distribution of the nanofibrils ranged from 5 up to 21 nm for NFC from POB and from 2 to 15 nm for NFC from POL. Different nano-composite materials using the NFC were also prepared by casting and evaporating a mixture of this suspension with acrylic based dispersion in natural rubber (NR) matrix. The effect of NFC loading on mechanical and thermal properties confirmed the potential use of *Posidonia* as a source for the production of NFC. The ensuing NFC from POB as well as POL demonstrated high reinforcing potential when incorporated into a polymer matrix.

Acknowledgments

The authors gratefully express their sincere gratitude to Prof. Mohamed Naceur Belgacem, Director of PAGORA–INP Grenoble, France, for his help and availability, as well as to the "PHC-UTIQUE CMCU" (project 13G 1114) and "SSHN 2014 – L'Institut Français de Tunisie" for their financial support.

References

Abe, K., Yano, H., 2009. Comparison of the characteristics of cellulose microfibril aggregates of wood, rice straw and potato tuber. Cellulose 16 (6), 1017–1023.
Abe, K., Iwamoto, S., Yano, H., 2007. Obtaining cellulose nanofibers with a uniform width of 15 nm from wood. Biomacromolecules 8 (10), 3276–3278.
Abrantes, S., Amaral, M.E., Costa, A.P., Duarte, A.P., 2007. *Cynara cardunculus* L. alkaline pulps: alternative fibres for paper and paperboard production. Bioresour. Technol. 98, 2873–2878.
Aguir, C., Mhenni, M.F., 2006. Experimental study on carboxymethylation of cellulose extracted from *Posidonia oceanica*. J. Appl. Polym. Sci. 98, 1808–1816.
Aguir, C., Mhenni, M.F., 2007. Removal of basic blue 41 from aqueous solution by carboxymethylated *Posidonia oceanica*. J. Appl. Polym. Sci. 103, 1215–1225.
Alemdar, A., Sain, M., 2008. Biocomposites from wheat straw nanofibers: morphology, thermal and mechanical properties. Compos. Sci. Technol. 68, 557–565.
Alila, S., Besbes, I., Vilar, M.R., Mutjé, P., Boufi, S., 2013. Non-woody plants as raw materials for production of microfibrillated cellulose (NFC): a comparative study. Ind. Crops Prod. 41 (1), 250–259.
Andresen, M., Johansson, L.S., Tanem, B.S., Stenius, P., 2006. Properties and characterization of hydrophobized nanofibrillar cellulose. Cell 13, 665–677.
Andresen, M., Stenius, P., 2007. Water-in-oil emulsions stabilized by hydrophobized nanofibrillar cellulose. J. Dispersion Sci. Technol. 28, 837–844.
Antunes, A., Amaral, E., Belgacem, M.N., 2000. *Cynara cardunculus* L.: chemical composition and Soda-Anthraquinone cooking. Ind. Crops Prod. 12, 85–91.
Belgacem, M.N., Zid, M., Nicolski, S.N., Obolenskaya, A.V., 1986. Study of the chemical composition of alpha from Tunisia. Chim. Technol. Drev. Mej. Sbor. Trud. 8, 111–114.
Bendahou, A., Habibi, Y., Kaddami, H., Dufresne, A., 2009. Physico-chemical characterization of palm from *Phoenix dactylifera*–L, P reparation of cellulose whiskers and natural rubber-based nanocomposites. J. Biobased Mater. Bioenergy 3, 81–90.
Bendahou, A., Kaddami, H., Dufresne, A., 2010. Investigation on the effect of cellulosic nanoparticles' morphology on the properties of natural rubber based nanocomposites. Eur. Polym. J. 46 (4), 609–620.
Benhamou, K., Dufresne, A., Magnin, A., Mortha, G., Kaddami, H., 2014. Control of size and viscoelastic properties of nanofibrillated cellulose from palm tree by varying the TEMPO-mediated oxidation time. Carbohydr. Polym. 99, 74–83.
Besbes, I., Rei Vilar, M., Boufi, S., 2011a. Nanofibrillated cellulose from alfa, eucalyptus and pine fibres: preparation, characteristics and reinforcing potential. Carbohydr. Polym. 86, 1198–1206.
Besbes, I., Alila, S., Boufi, S., 2011b. Nanofibrillated cellulose from TEMPO-oxidized eucalyptus fibres: effect of the carboxyl content. Carbohydr. Polym. 84, 975–983.
Bhattacharya, D., Germinario, L.T., Winter, W.T., 2008. Isolation: preparation and characterization of cellulose microfibers obtained from bagasse. Carbohydr. Polym. 73, 371–377.
Boufi, S., Gandini, A., 2015. Triticale crop residue: a cheap material for high performance nanofibrillated cellulose. RSC Adv. 5, 3141–3151.

Bruce, D.M., Hobson, R.N., Farrent, J.W., Hepworth, D.G., 2005. High-performance composites from low-cost plant primary cell walls. Compos. Part A Appl. Sci. Manuf. 36, 1486–1493.
Chaker, A., Mutjé, P., Rei Vilar, M., Boufi, S., 2014a. Agriculture crop residues as a source for the production of nanofibrillated cellulose with low energy demand. Cellulose 21, 4247–4259.
Chaker, A., Alila, S., Mutjé, P., Rei Vilar, M., Boufi, S., 2014b. Key role of the hemicellulose content and the cell morphology on the nanofibrillation effectiveness of cellulose pulps. Cellulose 20, 2863–2875.
Chakraborty, A., Sain, M., Kortschot, M., 2005. Cellulose microfibrals: a novel method of preparation using high shear refining and cryocrushing. Holzforschung 59, 102–107.
Chia, C.H., Zakaria, S., Nguyen, K.L., Abdullah, M., 2008. Utilisation of unbleached kenaf fibres for the preparation of magnetic paper. Ind. Crops Prod. 28 (3), 333–339.
Cordeiro, N., Belgacem, M.N., Torres, I.C., Mourad, J.C.V.P., 2004. Chemical composition and pulping of banana pseudo-stems. Ind. Crops Prod. 19, 147–154.
Dinand, E., Chanzy, H., Vignon, M.R., 1996. Parenchymal cell cellulose from sugar beet pulp: preparation and properties. Cellulose 3, 183–188.
Douissa, N., Bergaoui, L., Mansouri, S., Khiari, R., Mhenni, M.F., 2013. Macroscopic and microscopic studies of methylene blue sorption onto extracted celluloses from *Posidonia oceanica*. Ind.Crops Prod. 45, 106–113.
Dinand, E., Chanzy, H., Vignon, R.M., 1999. Suspensions of cellulose microfibrils from sugar beet pulp. Food Hydrocolloids 13 (3), 275–283.
Djafari Petroudy, S.R., Syverud, K., Chinga-Carrasco, G., Ghasemain, A., Resalati, H., 2014. Effects of bagasse microfibrillated cellulose and cationic polyacrylamide on key properties of bagasse paper. Carbohydre Polym. 99, 311–318.
Dufresne, A., Dupeyre, D., Vignon, M.R., 2000. Cellulose microfibrils from potatotuber cells: processing and characterization of starch-cellulose microfibril composites. J. Appl. Polym. Sci. 76, 2080–2092.
Dufresne, A., Cavaille, J.Y., Vignon, M.R., 1997. Mechanical behavior of sheets prepared from sugar beet cellulose microfibrils. J. Appl. Polym. Sci. 64, 1185–1194.
Dufresne, A., 2012. Nanocellulose From Nature to High-Performance Tailored Materials. de Gruyter.
Dufresne, A., 2010. Processing of polymer nanocomposites reinforced with polysaccharide nanocrystals. Mol. J. 15, 4111–4128.
Dutt, D., Upadhyaya, J.S., Malik, R.S., Tyagi, C.H., 2005. Studies on the pulp and papermaking characteristics of some Indian non-woody fibrous raw materials. Cellul. Chem. Technol. 39 (1–2), 115–128.
Dutt, D., Upadhyaya, J.S., Tyagi, C.H., Kumar, A., Lal, M., 2008. Studies on *Ipomea carnea* and *Cannabis sativa* as an alternative pulp blend for softwood: an optimization of kraft delignification process. Ind. Crops Prod. 28, 128–136.
Erkisen, O., Syverud, K., Gregersen, O., 2008. The use of microfibrillated cellulose produced from kraft pulp as strength enhancer in TMP paper. Nord. Pulp Paper Res. J. 23, 299–304.
Fukuzumi, H., Saito, T., Iwata, T., Kumamoto, Y., Isogai, A., 2009. Transparent and high gas barrier films of cellulose nanofibers prepared by TEMPO-mediated oxidation. Biomacromolecules 10 (1), 162–165.
Ganikhanov, F., Carrasco, S., Sunney Xie, X., 2006. Broadly tunable dual-wavelength light source for coherent anti-stokes Raman scattering microscopy. Opt. Lett. 31 (9), 1292–1294.
Gezguez, I., Dridi-Dhaouadi, S., Mhenni, F., 2009. Sorption of yellow 59 on *Posidonia oceanica*, a non-conventional biosorbent: comparison with activated carbons. Ind. Crops Prod. 29 (1), 197–204.
Gousse, C., Chanzy, H., Cerrada, M.L., Fleury, E., 2004. Surface silylation of cellulose microfibrils: preparation and rheological properties. Polymer 45, 1569–1575.
Habibi, Y., Mahrouz, M., Vignon, M.R., 2009. Nanofibrillar cellulose from the peel of prickly pear fruits. Food Chem. 115, 423–429.
Habibi, Y., Vignon, M.R., 2008. Optimization of cellouronic acid synthesis by TEMPO-mediated oxidation of cellulose III from sugar beet pulp. Cellulose 15, 177–185.
Hassan, M.L., Mathew, A.P., Hassan, E.A., El-Wakil, N.A., Oksman, K., 2012. Nanofibers from bagasse and rice straw process optimization and properties. Wood Sci. Technol. 46, 193–205.
Hassan, M.L., Mathew, A.P., Hassan, E.A., Oksman, K., 2010. Effect of pretreatment of bagasse pulp on properties of isolated nanofibers and nanopaper sheets. Wood Fiber Sci. 43, 1–15.
Hedjazi, S., Kordsahia, O., Patt, R., Latibrai, A.J., Tschirner, U., 2008. Anthraquinone (AS/AQ) pulping of wheat straw and totally chlorine free (TCF) bleaching of pulps. Ind. Crops Prod. 62 (2), 142–148.
Herrick, F.W., Casebier, R.L., Hamilton, J.K., Sandberg, K.R., 1983. Nanofibrillar cellulose: morphology and accessibility. J. Appl. Polym. Sci. 37, 797–813.
Imai, T., Putaux, J.L., Sugiyama, J., 2003. Geometric phase analysis of lattice images from algal cellulose microfibrils. Polymer 44, 1871–1879.
Isogai, A., Usuda, M., Kato, T., Uryu, T., Atalla, R.H., 1989. Solid-state CP/MAS carbon-13 NMR study of cellulose polymorphs. Macromolecules 22 (7), 3168–3172.
Iwamoto, S., Abe, K., Yano, H., 2008. The effect of hemicelluloses on wood pulp nanofibrillation and nanofiber network characteristics. Biomacromolecules 9, 1022–1026.
Iwamoto, S., Nakagaito, A.N., Yano, H., Nogi, M., 2005. Optically transparent composites reinforced with plant fibers-based nanofibers. Appl. Phys. A–Mater. 81, 1109–1112.
Janardhnan, S., Sain, M., 2006. Isolation of cellulose microfibrils–an enzymatic approach. Bioresources 1, 176–188.
Jang, J.H., Lee, S.H., Endo, T., Kim, N.H., 2013. Characteristics of microfibrillated cellulosic fibers and paper sheets from Korean white pine. Wood Sci. Technol. 47, 925–937.
Jonoobi, M., Khazaeian, A., Tahir, P.M., Azry, S.S., Oksman, K., 2011. Characteristics of cellulose nanofibers isolated from rub-berwood and empty fruit bunches of oil palm using chemo-mechanical process. Cellulose 18, 1085–1095.
Kalia, S., Boufi, S., Celli, A., Kango, S., 2014. Nanofibrillated cellulose: surface modification and potential applications. Colloid Polym. Sci. 292, 5–31.
Khiari, R., Mhenni, M.F., Belgacem, M.N., Mauret, E., 2010. Chemical composition and pulping of date palm rachis and *Posidonia oceanica* – a comparison with other wood and non-wood fibre sources. Bioresour. Technol. 101, 775–780.
Khiari, R., Marrakchi, Z., Belgacem, M.N., Mauret, E., Mhenni, M.F., 2011a. New lignocellulosic fibres-reinforced composite materials: a step forward in the valorisation of the *Posidonia oceanica* balls. Compos. Sci. Technol. 71, 187–1867.
Khiari, R., Mauret, E., Belgacem, M.N., Mhenni, F., 2011b. Tunisian date palm rachis used as an alternative source of fibres for papermaking applications. Bioresources 6, 265–281.
Klemm, D., Heublein, B., Fink, H.P., Bohn, A., 2005. Cellulose: fascinating biopolymer and sustainable raw material. Angew. Chem. Int. Ed. 44 (22), 3358–3393.
Liu, R.G., Yu, H., Huang, Y., 2005. Structure and morphology of cellulose in wheat straw. Cellulose 12 (1), 25–34.
Malainine, M.E., Mahrouz, M., Dufresne, A., 2005. Thermoplastic nanocomposites based on cellulose microfibrils from *Opuntia ficus-indica* parenchyma cell. Compos. Sci. Technol. 65, 1520–1526.
Moran, J.I., Alvarez, V.A., Cyras, V.P., Vazquez, A., 2008. Extraction of cellulose and preparation of nanocellulose from sisal fibers. Cell 15, 149–159.
Nakagaito, A.N., Yano, H., 2004. The effect of morphological changes from pulp fiber towards nano-scale fibrillated cellulose on the mechanical properties of high-strength plant fiber based composites. Appl. Phys. A–Mater. Sci. Process. 78, 547–552.
Ncibi, M.C., Mahjoub, B., Seffen, M., 2006a. Studies on the biosorption of textile dyes from aqueous solutions using *Posidonia oceanica* leaf sheath fibres. Adsorpt. Sci. Technol. 24 (6), 461–473.
Ncibi, M.C., Mahjoub, B., Seffen, M., 2006b. Biosorption of Phenol onto *Posidonia oceanica* seagrass in batch systems: equilibrium and kinetic modelling. Can. J. Chem. Eng. 84 (4), 495–500.
Ncibi, M.C., Altenor, S., Seffen, M., Brouers, F., Gaspard, S., 2008. Modelling single compound adsorption onto porous and non-porous sorbents using deformed Weibull exponential isotherm. Chem. Eng. J. 145 (2), 196–292.
Oh, S.Y., Yoo, D.I., Shin, Y., Kim, H.C., Kim, H.Y., Chung, Y.S., Park, W.H., Youk, J.H., 2005. Crystalline structure analysis of cellulose treated with sodium hydroxide and carbon dioxide by means of X-ray diffraction and FTIR spectroscopy. Carbohydr. Res. 340 (15), 2376–2391.
Rezayati Charani, P., Dehghani-Firouzabadi, M., Afra, E., Blademo, Å., Naderi, A., Lindström, T., 2013. Production of microfibrillated cellulose from unbleached kraft pulp of kenaf and Scotch pine and its effect on the properties of hardwood kraft microfibrillated cellulose paper. Cellulose 20, 2559–2567.
Rondeau-Mouro, C., Bouchet, B., Pontoire, B., Robert, P., Mazoyer, J., Buléon, A., 2003. Structural features and potential texturising properties of lemon and maize cellulose microfibrils. Carbohydr. Polym. 53, 241–252.
Rosli, W., Leh, W.D., Zainuddin, C.P., Tanaka, Z., 2003. Optimisation of soda pulping variables for preparation of dissolving pulps from oil palm fibre. Holzforschung 57 (1), 106–113.
Saito, T., Nishiyama, Y., Putaux, J.L., Vignon, M., Isogai, A., 2006. Homogeneous suspensions of individualized microfibrils from TEMPO-catalyzed oxidation of native cellulose. Biomacromolecules 7, 1687–1691.
Segal, L., Creely, J.J., Martin, A.E., Conrad, C.M., 1959. An empirical method for estimating the degree of crystallinity of native cellulose using the X-ray diffractometer. Text. Res. J. 29, 786–794.
Siqueira, G., Tadokoro, S.K., Mathew, A.P., Oksman, K., 2010a. Carrot nanofibers and nanocomposites applications, presented at the 7th International Symposiumon. In: Natural Polymers and Composites September 7–10, Gramado, Brazil.
Siqueira, G., Tapin-Lingua, S., Bras, J., Da Silva Perez, D., Dufresne, A., 2010b. Morphological investigation of nano-particles obtained from combined mechanical shearing, and enzymatic and acid hydrolysis of sisal fibers. Cellulose 17 (6), 1147–1158.
Siró, I., Plackett, D., 2008. Characterization of nanofibrillar cellulose (NFC) films made of different types of raw material. In: Nordic Polymer Days, 11–13 June, Stockholm, Sweden.
Stenstad, P., Andresen, M., Tanem, B.S., Stenius, P., 2008. Chemical surface modifications of nanofibrillar cellulose. Cell 15, 35–45.
Subramanian, R., Knononov, A., Kang, T., Paltakari, J., Paulapura, H., 2008. Natural cellulosic fibrils. Bioresources 3, 192–203.
Syverud, K., Stenius, P., 2009. Strench and barrier properties of NFC films. Cell 16, 75–85.
Turbak, A.F., Snyder, F.W., Sandberg, K.R., 1983. Nanofibrillar cellulose a new cellulose product: properties, uses, and commercial potential. J. Appl. Polym. Sci. 37, 815–827.
Wang, B., Mohini, S., 2007. Isolation of nanofibers from soybean source and their reinforcing capability on synthetic polymers. Compos. Sci. Technol. 67, 2521–2527.

Please cite this article in press as: Bettaieb, F., et al., Nanofibrillar cellulose from *Posidonia oceanica*: Properties and morphological features. Ind. Crops Prod. (2015), http://dx.doi.org/10.1016/j.indcrop.2014.12.060

Winuprasith, T., Suphantharika, M., 2013. Microfibrillated cellulose from mangosteen (*Garcinia Mangostana* L.) rind Preparation characterization, and evaluation as an emulsion stabilizer. Food hydrocolloid 32, 383–394.
Zhang, J., Song, H., Lin, L., Zhuang, J., Pang, C., Liu, S., 2012. Microfibrillated cellulose from bamboo pulp and its properties. Biomass Bioenergy 39, 78–83.
Zhao, H.P., Feng, X.Q., Gao, H., 2007. Ultrasonic technique for extracting nanofibres from nature materials. Appl. Phys. Lett. 90, 073–112.
Zuluaga, R., Putaux, J.L., Cruz, J., Vélez, J., Mondragon, I., Gañán, P., 2009. Cellulose microfibrils from banana rachis: effect of alkaline treatments on structural and morphological features. Carbohydr. Polym. 76 (1), 51–59.

Please cite this article in press as: Bettaieb, F., et al., Nanofibrillar cellulose from *Posidonia oceanica*: Properties and morphological features. Ind. Crops Prod. (2015), http://dx.doi.org/10.1016/j.indcrop.2014.12.060